Supporting Information

Bamboo Derived N-doped Carbon as a Bifunctional Electrode for High-performance Zinc-air Batteries

Peng Cui,‡[a] Tingzhen Li,‡[a] Xiao Chi,‡[a] Wu Yang,[a] Zehong Chen,[a] Wenjia Han,[b] Ruidong Xia,[c] Shimelis Admassie,[d] Emmanuel Iheanyichukwu Iwuoha,[e] and Xinwen Peng[a]*

[a] State Key Laboratory of Pulp and Paper Engineering, South China University of Technology, Guangzhou, China, 510640

[b] State Key Laboratory of Biobased Material and Green Papermaking, Qilu University of Technology (Shandong Academy of Sciences), Jinan, China, 250353

[c] School of Materials Science and Engineering, Nanjing University of Posts and Telecommunications, Nanjing, China, 210023

[d] Department of Chemistry, Addis Ababa University, PO Box 1176, Addis Ababa, Ethiopia

[e] Key Laboratory for NanoElectrochemistry, 4th Floor Chemical Sciences Building, University of the Western Cape, Robert Sobukwe Road, Bellville 7535, Cape Town, South Africa

Supplementary Figures and Tables

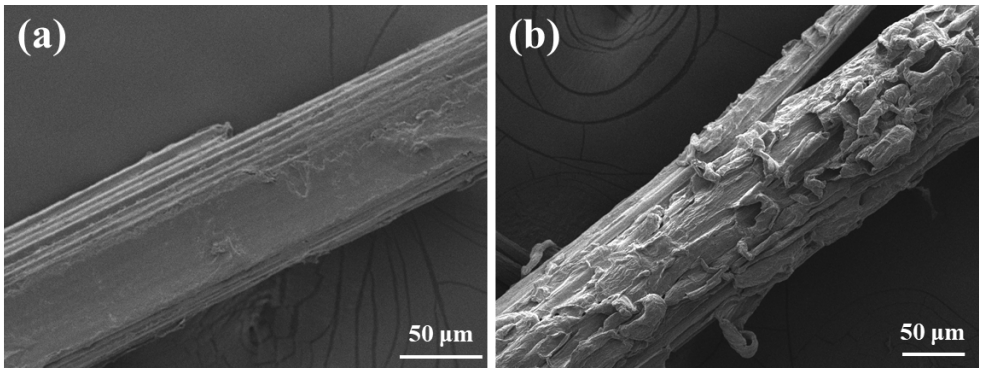

Figure S1. SEM of (a) bamboo sliver before and (b) after pretreatment.

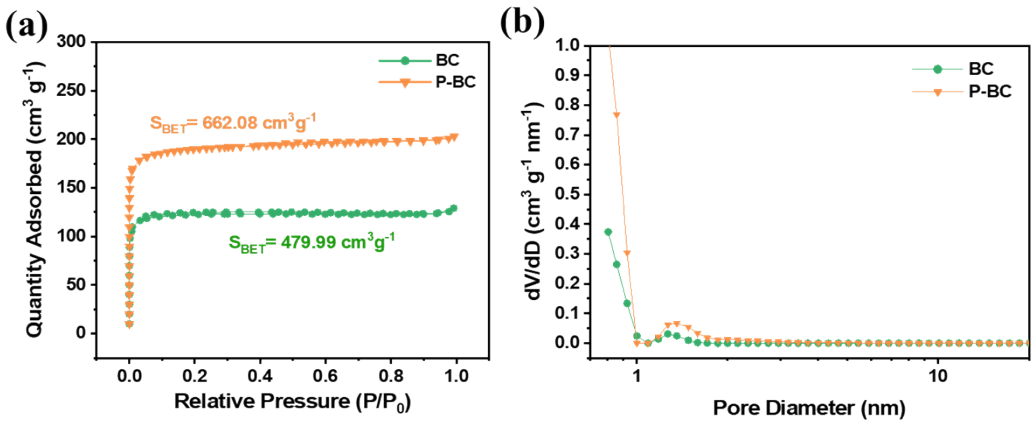

Figure S2. (a) BET N_2 adsorption/desorption isotherms and (b) DFT pore size distribution curves of BC and P-BC.

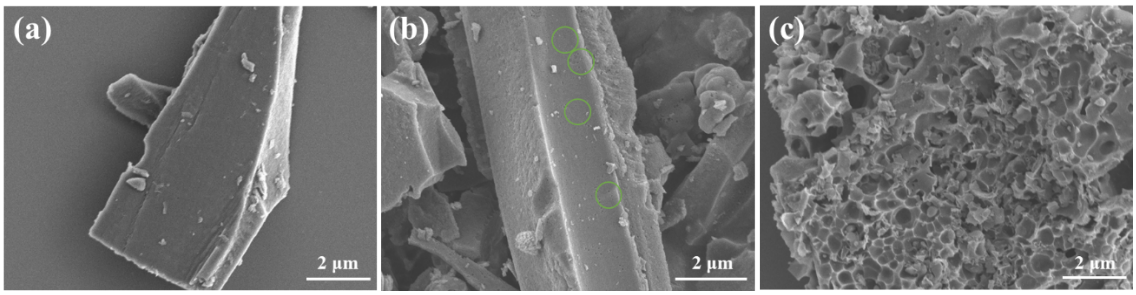

Figure S3. SEM under high magnification of (a) BC and (b) NBC (c) NPBC after grinding.

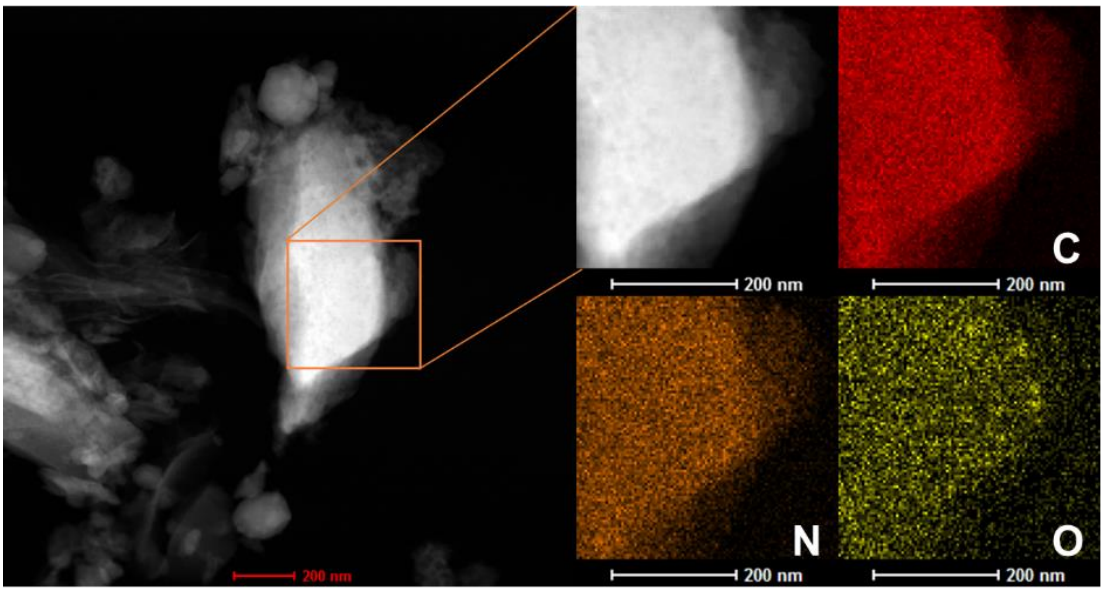

Figure S4. HAADF-STEM and corresponding EDS elemental mapping images for C, N, and O of NPBC.

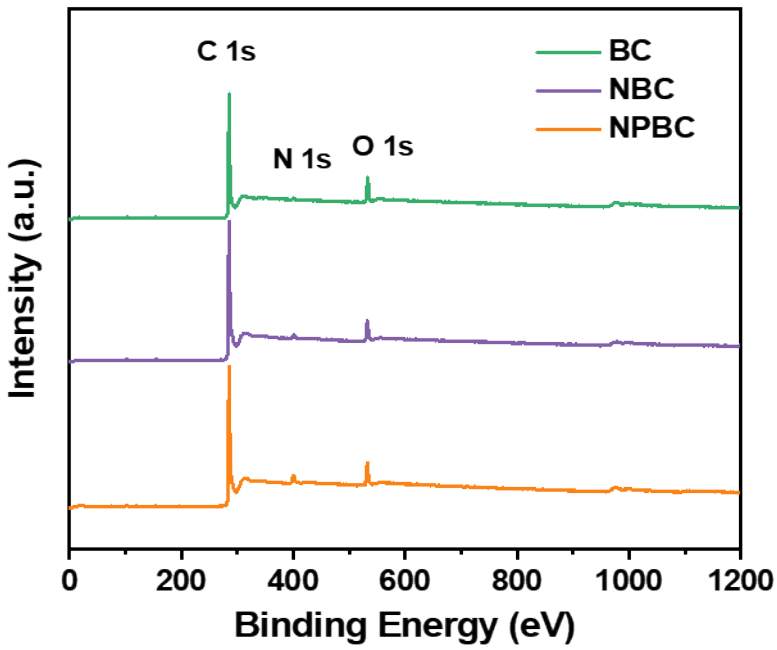

Figure S5. XPS survey spectra of BC, NBC, and NPBC.

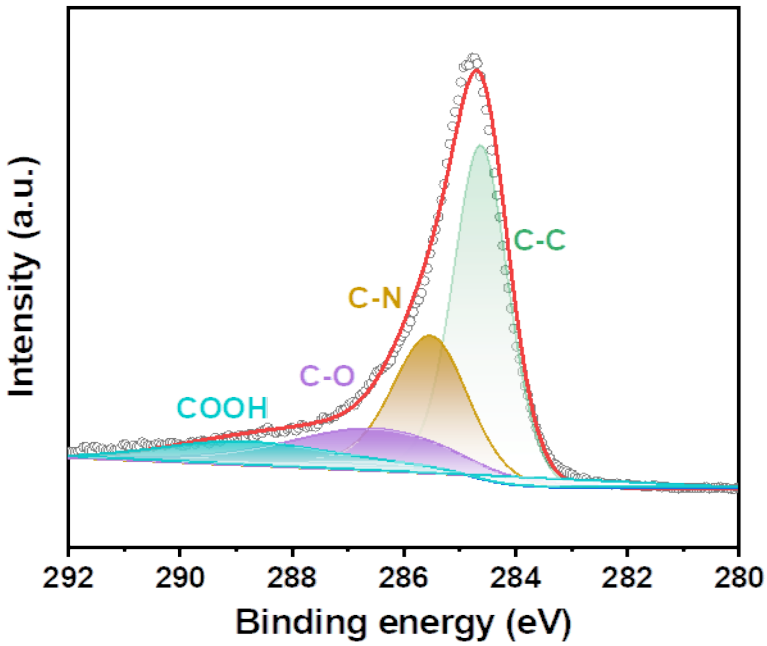

Figure S6. The high-resolution C 1s spectra of NPBC.

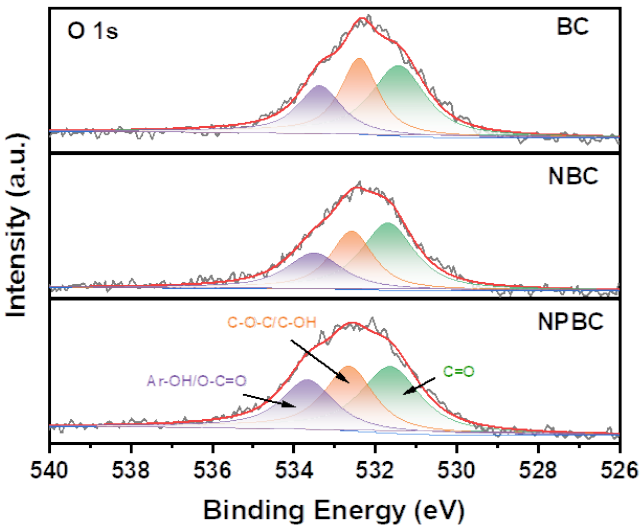

Figure S7. The high-resolution O 1s spectra of BC, NBC and NPBC. In the high-resolution XPS spectrum of O 1s, three peaks in all samples at binding energies of 531.3, 532.6 and 533.5 eV are indexed to C=O aromatic carbonyl groups, C-OH hydroxylic groups or C-O-C ether groups and Ar-OH aromatic alcohols or O-C=O ester groups, respectively.

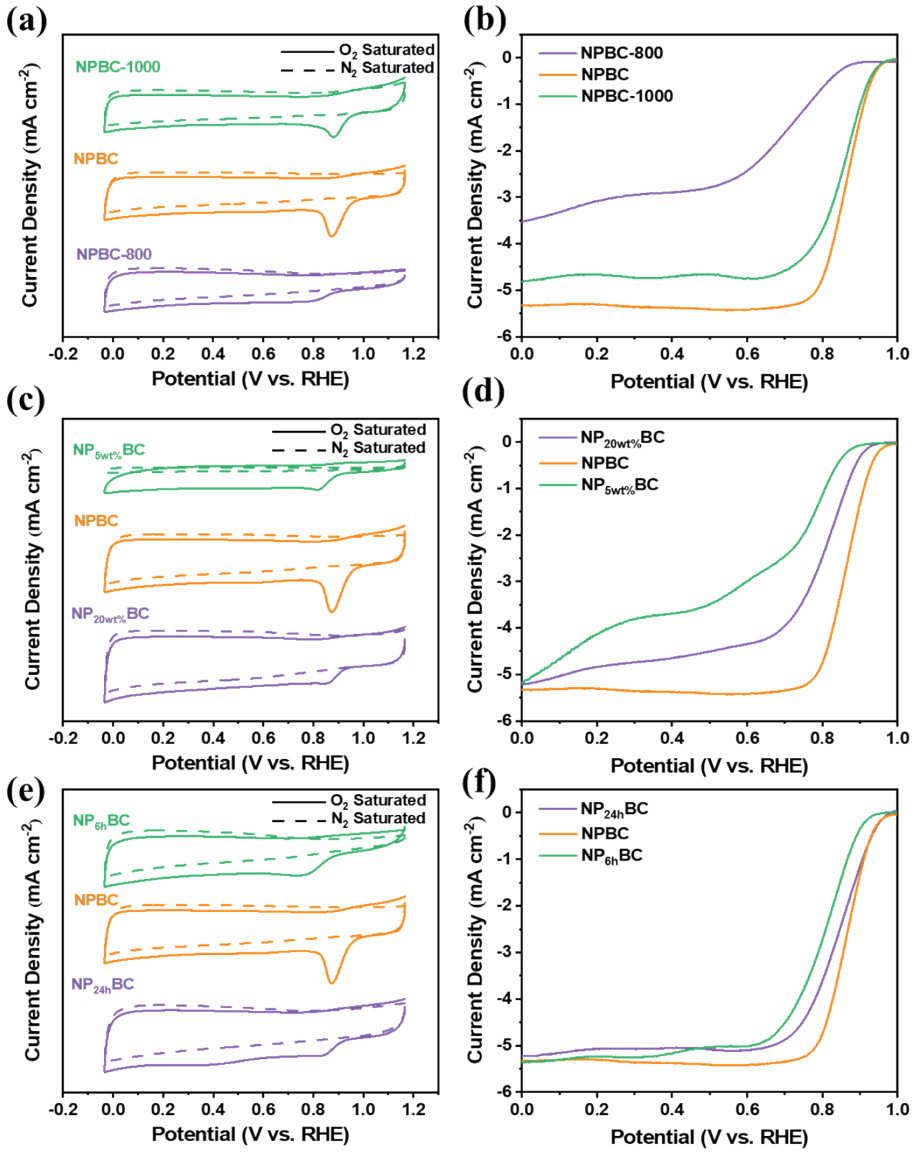

Figure S8. Comparison of CV and LSV of samples under different treatment conditions (NP_XBC-T, X means the concentration of sodium hydroxide or pretreatment time, T means the carbonization temperature).

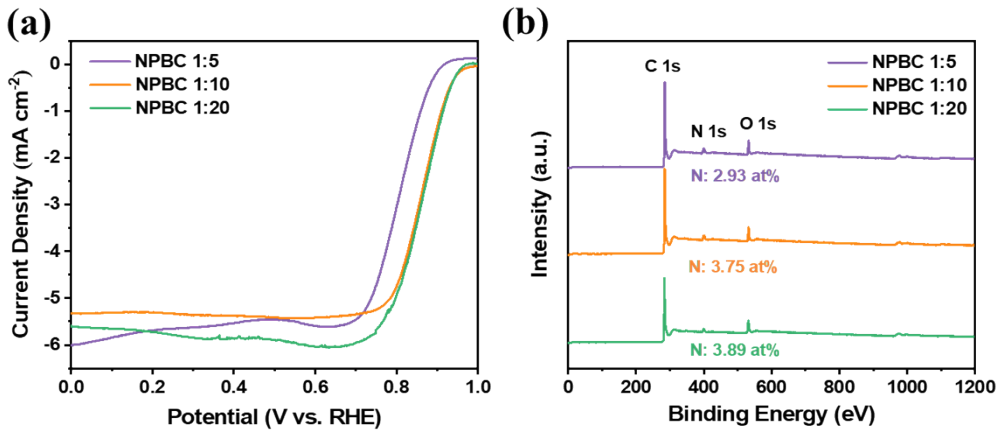

Figure S9. (a) LSV and (b) XPS survey spectra of materials prepared with different ratios of ammonium chloride.

As shown in Figure S9, We found that after increasing the amount of NH_4Cl (1:20), the N content of the catalyst did not show a substantial increase, and also the catalytic performance (E_{onset}, $E_{1/2}$) did not improve greatly. Therefore, it is better to use a ratio of 1:10 in order to be greener and conserve resources.

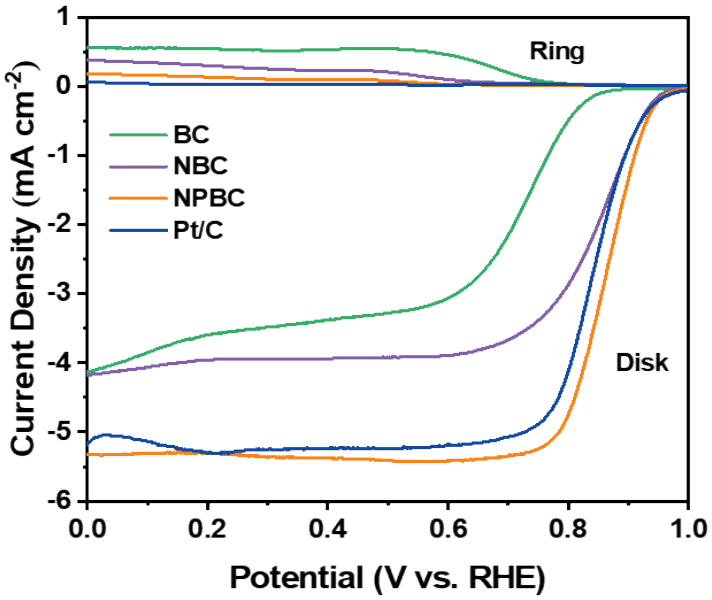

Figure S10. (a) RRDE curves of all samples.

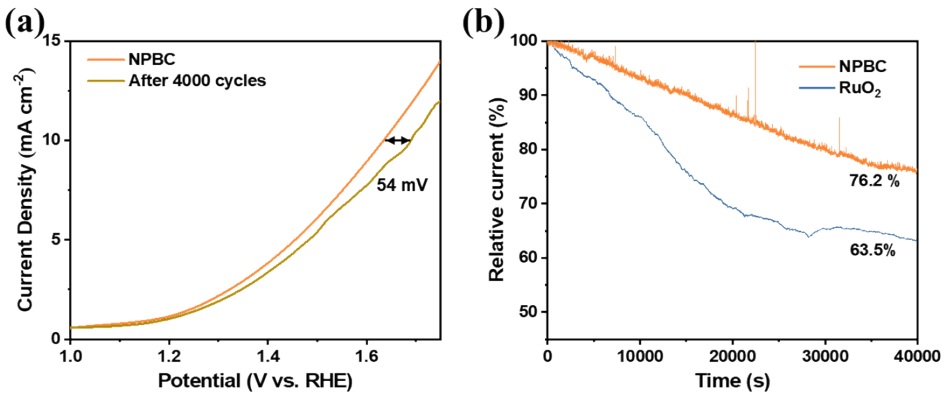

Figure S11. (a) the OER performance of the catalyst after Adt; (b) Chronoamperometric responses of the NPBC and RuO_2 at 1.5 V.

The CV accelerating durability tests (ADT) were conducted at a scanning rate of 50 mV s^{-1} from 1 to 1.6 V in an O_2-saturated 0.1 M KOH solution. After 4000 cycles, the OER overpotential of NPBC increased by 54 mV. In addition, after chronoamperometry tests for 40000 s, NPBC displays a current retention of 76.2 %, which is higher than that of benchmark RuO_2 catalyst (63.5 % current retention).

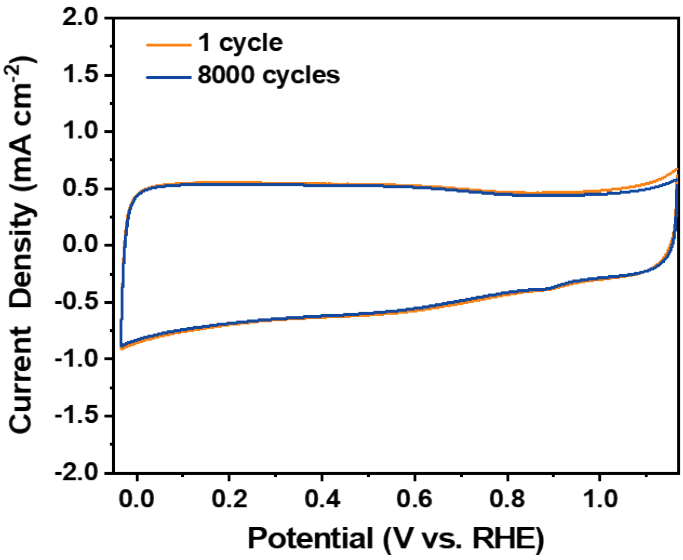

Figure S12. CV curves different CV cycles in an N_2-saturated 0.1M KOH aqueous solution.

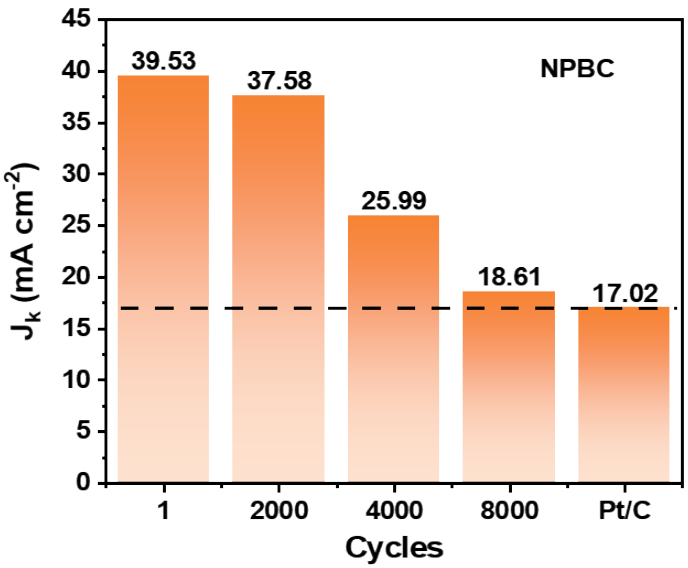

Figure S13. The kinetic current density (J_k) calculated after ADT.

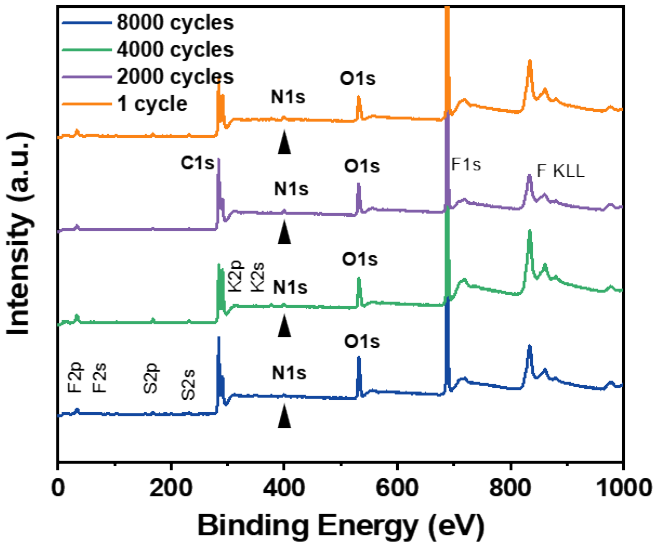

Figure S14. XPS survey spectra of NPBC after different cycles of CV scans. (C, N, and O elements can be clearly identified, while F, S, and K elements may come from residual Nafion and KOH).

Figure S15. Image of the ZAB with a measure open-circuit voltage of 1.46 V.

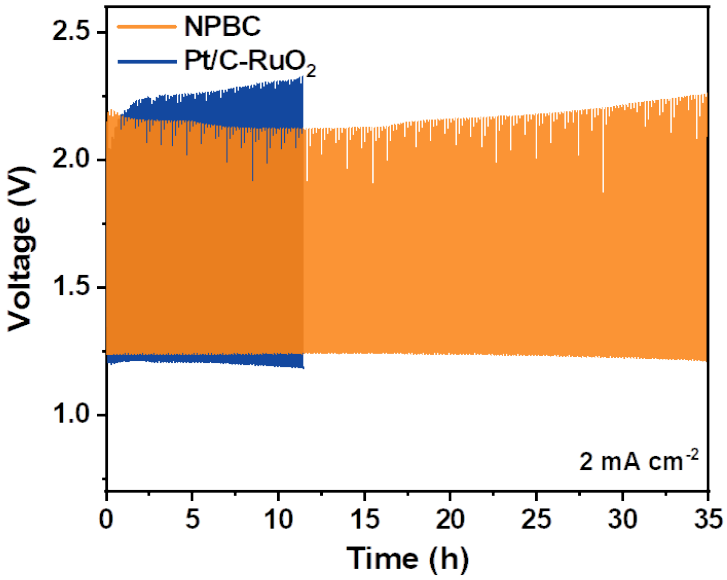

Figure S16. Charge-discharge curves cycling curves of ZABs with NPBC and Pt/C+RuO_2 at 2 mA cm^{-2}.

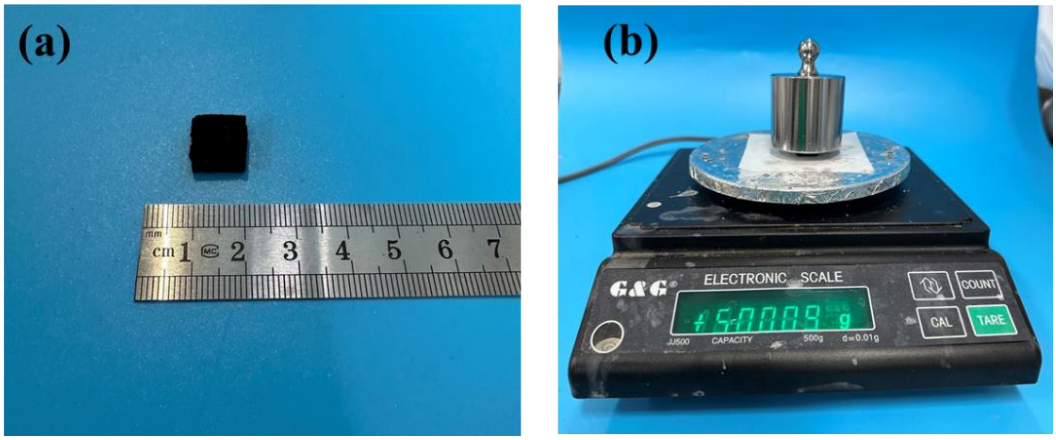

Figure S17. (a) Digital photographs of NPBC in the size of 1*1*0.4 cm, and (b) its image supporting 500g of weight.

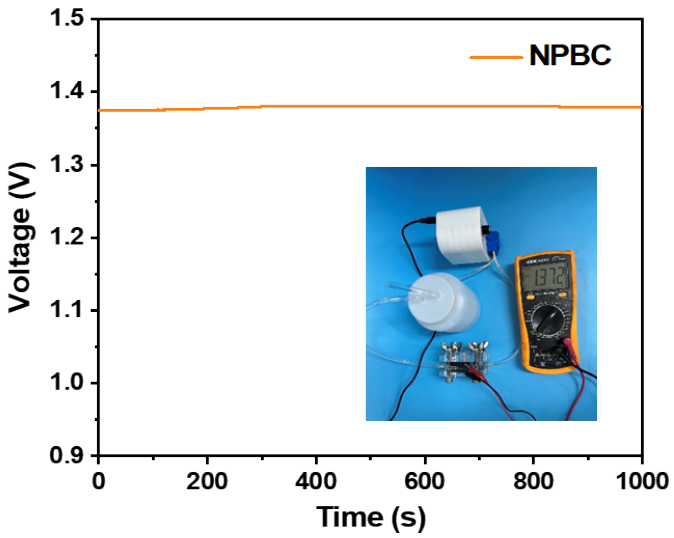

Figure S18. Open-circuit curve and image (insert) of the liquid flow ZABs with NPBC.

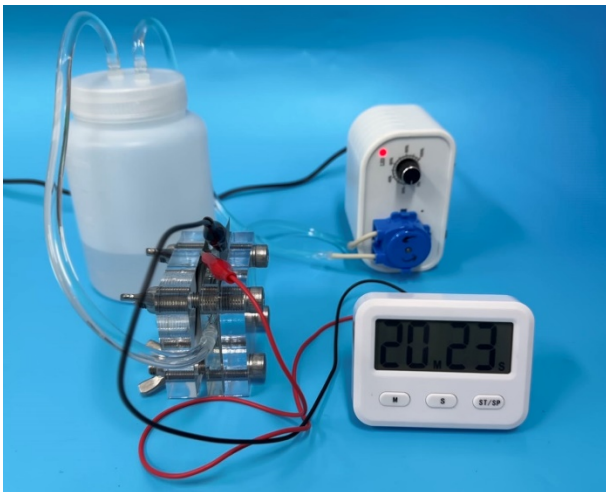

Figure S19. An electronic clock powered by a liquid flow ZAB.

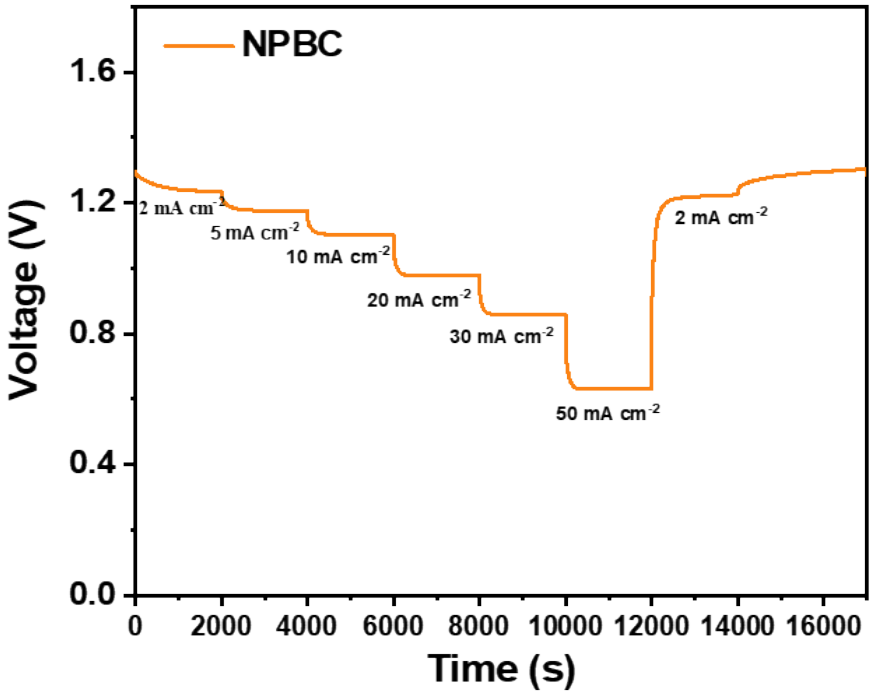

Figure S20. Galvanostatic discharge curves of the liquid flow ZAB with NPBC.

Table S1. Specific surface area (SSA) and pore structure of all samples.

Sample	S_{BET} (m^2 g^{-1})	Pore volume (cm^3 g^{-1})	Pore diameter (nm)
BC	479.99	0.20	1.66
NBC	532.21	0.21	1.62
NPBC	745.12	0.51	2.72

Table S2. Elemental contents of samples obtained from XPS.

Sample	Atomic content (%)						
	C	O	N				
			Pyridinic-N	Pyrrolic-N	Graphitic-N	Oxidized-N	Total
BC	91.68	8.32	—	—	—	—	—
NBC	89.31	7.98	0.52	0.73	0.73	0.74	2.72
NPBC	86.54	9.71	0.88	0.89	1.08	0.88	3.75

Table S3. Summary of the reported ORR performance of NC-MFCs electrocatalysts.

Catalyst	E_{onset}	$E_{1/2}$	Ref.
NPBC	0.98	0.864	**This work**
NBCNT-10	0.958	0.82	1
NCF	1.0	0.85	2
NPCS-900	0.99	0.87	3
CNS	0.97	0.87	4
N-CNF aerogel	-	0.80	5
HPNSC	0.98	0.87	6
PyN-GDY	1.0	0.84	7
N–S–Cs-900	-	0.84	8
ND-GLC	0.991	0.875	9
S-g-C_3N_4/P123	-	0.863	10

Table S4. Summary of the reported ORR and OER performance of NC-MFCs electrocatalysts.

Catalyst	$E_{1/2}$	$E_{j=10}$	$\triangle E$ ($E_{j=10}$ - $E_{1/2}$)	Ref.
NPBC	0.864	1.644	0.780	**This work**
NSP-Gra	0.82	1.76	0.94	11
CA-1/10-900°C	0.821	1.757	0.936	12
HHPC	0.78	1.58	0.80	13
P,S-CNS	0.87	1.56	0.69	14
PS-CNF	0.86	1.55	0.69	15
NKCNPs-900	0.79	1.71	0.92	16
NPF-CNS-2	0.81	1.57	0.76	17
$BRC_{AC}850_2$	0.85	1.68	0.83	18
CNT@NSC	0.82	1.56	0.74	19
NPCNFs-O	0.85	1.566	0.716	20

REFERENCES

1. P. Wei, X. Li, Z. He, X. Sun, Q. Liang, Z. Wang, C. Fang, Q. Li, H. Yang, and J. Han, *Chem. Eng. J.*, 2021, **422,** 130134.
2. L. Zhang, T. Gu, K. Lu, L. Zhou, D. S. Li, and R. Wang, *Adv. Funct. Mater.*, 2021, **31**, 2103187.
3. G. Ren, S. Chen, J. Zhang, N. Zhang, C. Jiao, H. Qiu, C. Liu and H. L. Wang, *J. Mater. Chem. A*, 2021, **9**, 5751-5758.
4. S. Cao, W. Shang, G. L. Li, Z. F. Lu, X. Wang, Y. Yan, C. Hao, S. Wang and G. Sun, *Carbon*, 2021, **184**, 127-135.
5. H. W. Liang, Z. Y. Wu, L. F. Chen, C. Li and S. H. Yu, *Nano Energy*, 2015, **11**, 366-376.
6. Y. Cheng, Y. Wang, Q. Wang, Z. Liao, N. Zhang, Y. Guo and Z. Xiang, *J. Mater. Chem. A*, 2019, **7**, 9831-9836.
7. Q. Lv, N. Wang, W. Si, Z. Hou, X. Li, X. Wang, F. Zhao, Z. Yang, Y. Zhang and Huang, C. *Appl. Catal. B*, 2020, **261**, 118234.
8. L. Xing, C. Song and A. Kong, *J. Solid State Chem.*, 2020, **287**, 121348.
9. J. Zhang, Y. Sun, J. Zhu, Z. Kou, P. Hu, L. Liu, S. Li, S. Mu and Y. Huang, *Nano Energy*, 2018, **52**, 307-314.
10. X. B. Ding, F. Li, Q. C. Cao, H. Wu, Y. H. Qin, L. Yang, T. Wang, X. Zheng and C. W. Wang, *Chem. Eng. J.*, 2022, **429**, 132469.
11. Y. Wang, N. Xu, R. He, L. Peng, D. Cai and J. Qiao, Large-scale *Appl. Catal. B-Environ*, 2021, **285**, 119811.
12. H. Yabu, K. Ishibashi, M. S. Grewal, Y. Matsuo, N. Shoji and K. Ito, *Sci. Technol. Adv Mater.*, 2022, **23**, 31-40.
13. X. Xiao, X. Li, Z. Wang, G. Yan, H. Guo, Q. Hu, L. Li, Y. Liu and J. Wang, *Appl. Catal. B-Environ.*, 2020, **265**, 118603.
14. S. S. Shinde, C. H. Lee, A. Sami, D. H. Kim, S. U. Lee and J. H. Lee, *ACS nano*, 2017, **11**, 347-357.
15. S. S. Shinde, J. Y. Yu, J. W. Song, Y. H. Nam, D. H. Kim and J. H. Lee, *Nanoscale Horiz.*, 2017, **2**, 333-341.
16. Q. Wang, Y. Lei, Y. Zhu, H. Wang, J. Feng, G. Ma, Y. Wang, Y. Li, B. Nan and Q. Feng, *ACS appl. Mater. Interfaces*, 2018, **10**, 29448-29456.
17. Y. Zheng, H. Song, S. Chen, X. Yu, J. Zhu, J. Xu, K. A. Zhang, C. Zhang and T. Liu, *Small*, 2020, **16**, 2004342.
18. Q. Li, T. He, Y. Q. Zhang, H. Wu, J. Liu, Y. Qi, Y. Lei, H. Chen, Z. Sun and C. Peng, *ACS Sustainable Chem. Eng.*, 2019, **7**, 17039-17046.
19. X. Wang, G. L. Li, Z. F. Lu, S. Cao, C. Hao, S. Wang and G Sun, *Catal. Sci. Technol.*, 2022, **12**, 181-191.
20. F. Qiang, J. Feng, H. Wang, J. Yu, J. Shi, M. Huang, Z. Shi, S. Liu, P. Li and L. Dong, *ACS Catal.*, 2022, **12**, 4002-4015.